Comparative biophysical studies on the interaction of SPM and NASPM with DNA polynucleotides revealed the specificity and energetics of binding.

Probing the interaction of spermine and 1-naphthyl acetyl spermine with DNA polynucleotides: A comparative biophysical and thermodynamic investigation[†]

Ayesha Kabir and Gopinatha Suresh Kumar*

Biophysical Chemistry Laboratory, Chemistry Division, CSIR- Indian Institute of Chemical Biology, Kolkata 700 032, India

Correspondence to:

Dr. G. Suresh Kumar

Senior Principal Scientist**,** Biophysical Chemistry Laboratory

CSIR-Indian Institute of Chemical Biology

4, Raja S. C. Mullick Road, Kolkata 700 032, INDIA

Phone: +91 33 2472 4049, Fax: +91 33 2473 0284 / 5197

e-mail: gskumar@iicb.res.in/gsk.iicb@gmail.com

[†]Electronic supplementary information (ESI) available: Fig. S1,S2 and Tables S1,S2. See DOI:

2

Abstract

Interaction of spermine and its analogue, 1-naphthyl acetyl spermine with four double stranded DNA polynucleotides has been studied to understand the structural and thermodynamic basis of the binding. Efficacy and specificity of DNA binding with this analogue is not yet revealed. Energetics of the interaction was studied by isothermal titration calorimetry and differential scanning calorimetry. Circular dichroism spectroscopy, UV-thermal melting and ethidium bromide displacement assay have been employed to characterize the association. Circular dichroism studies showed that 1-naphthyl acetyl spermine caused stronger structural perturbation in the polynucleotides. Among the adenine-thymine polynucleotides the alternating polynucleotide was more preferred by naphthyl acetyl spermine compared to the preference of spermine for the homo sequence. The higher melting stabilization revealed from optical melting and differential scanning calorimetry results suggested that the binding of 1-naphthyl acetyl spermine increased the melting temperature and the total standard molar enthalpy of transition of adenine-thymine polynucleotides. Microcalorimetry results revealed that unlike spermine the binding of 1-naphthyl acetyl spermine was endothermic. The interaction was characterized by total enthalpy–entropy compensation and high standard molar heat capacity values. There are differences in the mode of association of 1-naphthyl acetyl spermine and spermine. 1-naphthyl acetyl spermine binds with an enhanced affinity with the adenine-thymine hetero polynucleotide. Thus, the result suggests importance of polyamine analogues and their ability to interfere with normal polyamine interactions.

Key words: Polyamines, Polyamine analogue, DNA Interaction, CD spectroscopy, Calorimetry, Thermodynamics

Introduction

Polyamines are polycationic alkyl amines that not only interact with an array of biological molecules but are also believed to play pivotal roles in maintaining cellular growth and activities.[1,2] Polyamine influenced dynamical bending of DNA molecules and induced DNA condensation, is reported to affect functionality of DNA interacting proteins and transcription of genes.[3,4] Polyamine concentration in malignant tumors is reported to be conspicuously higher than in normal cells.[5,6] This up regulation of polyamine concentration is due to the deterioration of polyamine metabolism which leads to the dysregulation of cell proliferation whereas decrease in the intracellular concentration of polyamines leads to inhibition of cellular growth and in many cases apoptosis.[7-9] Therefore, polyamine function and metabolism have been recognized as essential targets for anti-cancer and antiproliferative treatment.[10-13]

Inhibition of specific biosynthetic enzymes within the polyamine metabolic pathway have had remarkable potential to block tumor growth but this strategy is yet to have significant clinical success in the treatment of cancer.[12] The more recent approach has been to utilize the self-regulatory nature of polyamine metabolism by using polyamine analogues.[12,13] A number of polyamine analogues are being developed and many have showed strong cytotoxicity against tumor growth in a number of cell lines.[14-19] A good analogue might use the selective polyamine transporter to gain entry into the cell. In doing so it is competing with the natural polyamines for uptake and DNA binding. This phenomenon may thereby lead to down regulation of multiple polyamine biosynthetic enzymes and up regulation of polyamine catabolism resulting in decrease of intracellular polyamine concentration. Since the polyamine analogue does not substitute for the natural polyamines in growth accelerating function it exhibits selective anti-cancer cytotoxicity.[12,13,19]

Polyamines and analogues interact and stabilize a variety of double and triple stranded DNA and RNAs.[20-38] The mechanism of such interaction continues to evoke considerable interest and curiosity in understanding the antiproliferative activity.[39] The secondary amino groups in the polyamine chains play an essential role in these interactions which are suggestive of different hydrogen bonding modes other than electrostatic interactions.[25] As a result, polyamine structural analogues which have the ability to interfere with normal interactions have been proposed as a mechanism of cytotoxic activity.[12]

Thus, with regard to the recent turn of interest towards polyamine analogues, in this report, we have studied the comparative binding aspects of spermine (SPM) and spermine analogue, 1-naphthyl acetyl spermine (NASPM) with four DNA polynucleotides. NASPM (Fig. 1) is also a synthetic analogue of Joro spider toxin having long-lasting anticonvulsant effect on previously kindled rats.[40] Studies have also suggested that NASPM may be useful as a pharmacological tool for investigating physiological and pathological roles of AMPA receptors, and to develop new agents for the treatment of neuronal cell death and epilepsy.[41] Nucleic acid binding efficacy of this analogue is not yet revealed. Thus, proposing NASPM as an attractive polyamine analogue, biophysical studies on the interaction of NASPM with poly(dA).poly(dT), poly(dA-dT).poly(dA-dT), poly(dG).poly(dC) and poly(dG-dC).poly(dG-dC) were performed and compared to SPM to characterize the base specificity and, structural and energetic aspects of the interaction.

Results and Discussion

Comparative conformational changes induced by SPM and NASPM

The comparative effects of the polyamines SPM and NASPM on the circular dichroism spectra of the four polynucleotides was investigated. The results are depicted in Fig. 2. Note that both polyamines are optically inactive and do not have any CD spectra of their own, and the changes

can be solely attributed to structural changes in the polynucleotide conformation resulting from the interaction. The intrinsic CD spectrum of the poly(dA)·poly(dT) (AT homo polynucleotide) was characterized by a small positive peak at 259 nm, a negative peak at 247 nm and a positive peak at 220 nm (Spectrum 1 in Fig. 2A and B). The interaction of SPM and NASPM resulted in significant changes in the CD spectra. The positive and negative peaks in the 260-280 nm region reduced in intensity in both the cases. In the case of NASPM, the decrease in the 247 nm negative peak and the 220 nm positive peak intensity was also significant and it is worthy to note that an isoelliptic point was observed at 254 nm that was not observed with SPM.

The CD spectrum of poly(dA-dT).poly(dA-dT) (AT hetero polynucleotide) was characterized by a positive band around 264 nm followed by a negative band at 247 nm and a small positive peak around 225 nm (Spectrum 1 in Fig. 2C and D). In the presence of SPM and NASPM there were substantial changes of ellipticity of the 264 nm positive peak and minor changes in the negative peak at 247 and the positive peak at 225 nm. With SPM, the positive band ellipticity decreased (Fig. 2C). The interaction of NASPM (Fig. 2D) here is noteworthy; the change was more pronounced compared to SPM wherein there was a sharp increase in the ellipticity for the positive peak 264 nm accompanied by a concomitant red shift to 268 nm. Two isoelliptical points were registered at 264 and 240 nm, respectively, depicting the changes in the conformation to be in equilibrium with the original polynucleotide conformation. This observation leads to significant inference about the strong interaction between NASPM with the AT hetero polynucleotide.

The poly(dG).poly(dC) (GC homo polynucleotide) is characterized by a positive hump around 290 nm and a large positive peak at 256 nm followed by two negative peaks around 245 and 256

nms (Fig 2E and F). There was decrease in the ellipticity of the 256 nm peak in the presence of both SPM and NASPM. The change was more or less similar in both the cases.

The intrinsic spectrum of poly(dG-dC)·poly(dG-dC) (GC hetero polynucleotide) was characterized by a broad long wavelength positive band in the range of 275-285 nm with a peak around 281 nm followed by a negative peak around 252 nm (Fig. 2G and H). SPM binding enhanced the ellipticity of the long wavelength band leading to a sharp peak at 274 nm. NASPM binding lead to an increase in the ellipticity at 281 nm with the presence of two isoelliptic points at 270 and 262 nm, respectively. From the CD spectral data the changes on the interaction of NASPM with the DNA polynucleotides were of significance specially in the case of poly(dA-dT).poly(dA-dT). Also, the pattern of changes of CD signal on addition of both polyamines with the homo polynucleotides was of similar type, whereas different pattern for the interactions of NASPM with hetero AT and hetero GC polynucleotides was observed. These differences in pattern and intensity for the binding of NASPM to hetero polynucleotides indicate the binding mechanism to be different as compared to SPM. Also the difference in spectral data intensity for the different polynucleotides infers the binding to be sensitive towards base composition and sequence. Thus, from the CD spectral study we can propose sequence selectivity of NASPM towards the alternating AT sequences i.e. poly(dA-dT).poly(dA-dT).

Salt dependent CD studies for the interaction of SPM and NASPM with poly(dA-dT).poly(dA-dT) were conducted at 10 mM and 30 mM Na^+ concentration, respectively, and the data compared to the results obtained at 20 mM [Na^+]. At 10 mM Na^+ salt concentration, it was observed that for SPM, the positive band ellipticity decreased to a greater extent as compared to the change at 20 mM [Na^+]. However, at 30 mM [Na^+], there was a decrease in the change of band ellipticity. The % changes in the molar ellipticity of the bands at 10 mM, 20 mM and 30

mM [Na$^+$] were 48.6%, 39.2% and 31.9%, respectively. Similar results were also obtained for the interactions of NASPM to the DNA polynucleotides. Here the % change in the band molar ellipticity was greater at 10 mM and lesser at 30 mM. The % changes in the molar ellipticity of the bands at 10 mM, 20 mM and 30 mM [Na$^+$] were 39.4%, 23.2% and 17.8%, respectively. These results can be suggested to arise from the high electrostatic interactions between Na$^+$ ions and the DNA phosphate backbone. Increase in salt concentration leads to greater shielding of the DNA backbone which hinders the polyamines from binding to the DNA. Thus, it can be seen that conformational changes in the DNA polynucleotides were more pronounced at lower salt concentrations. This was also complemented from the greater change in intensity for the CD bands of the DNA-polyamine complexes. Therefore, this study gives valuable insights into the structural basis of these interactions that essentially depends on the salt concentration.

Thermodynamics of interaction of SPM and NASPM by isothermal titration calorimetry

The interaction of SPM and NASPM with the polynucleotides was studied by isothermal titration calorimetry. The ITC profiles for the interaction with the two AT polynucleotides are presented in Fig. 3. Each interaction was deduced to be monophasic i.e. there is only one binding event. The data were fitted to a model of single set of identical sites that yielded excellent fitting of the experimental data. The titration of SPM to poly(dA).poly(dT) resulted in negative peaks which revealed the binding to be exothermic (Fig, 3A). On the other hand, binding of SPM to poly(dA-dT).poly(dA-dT) was found to be endothermic (Fig. 3B). NASPM binding to both homo and hetero AT polynucleotides was endothermic (Fig. 3C,D). With the poly(dA).poly(dT), the binding affinity of SPM was 3.28×10^6 M^{-1} and that of NASPM was 1.15×10^6 M^{-1} . The binding affinity of the SPM and NASPM with poly(dA-dT).poly(dA-dT) were 8.20×10^5 M^1 and 2.12×10^6 M^{-1}, respectively. Thus, the affinity was highest for NASPM with hetero AT

polynucleotide and SPM with homo AT polynucleotide. In all the cases the negative standard molar Gibbs energy change confirmed spontaneous binding. The quantitative results obtained from the thermograms are summarized in Table 1.

Binding of SPM to poly(dG).poly(dC) showed negative peaks in the plot of power versus time, revealing the binding to be exothermic and to that of poly(dG-dC).poly(dG-dC) was found to be endothermic as shown in Fig. S1(ESI†). In both the systems interaction was observed to be higher for poly(dG).poly(dC) compared to poly(dG-dC).poly(dG-dC). The binding affinity values and the thermodynamic parameters are presented in Table S1 (ESI†). The interaction of NASPM with both GC polynucleotides was revealed to be exothermic. Binding affinity to poly(dG-dC).poly(dG-dC) was deduced to be 8.83×10^5 M^{-1} while that to poly(dG).poly(dC) was deduced to be 3.93×10^5 M^{-1} as shown in Table S1 (ESI†). SPM binding to poly(dA).poly(dT) showed the highest binding affinity, followed by poly(dA-dT).poly(dA-dT), poly(dG).poly(dC) and poly(dG-dC).poly(dG-dC) while the affinity of NASPM varied in the order, poly(dA-dT).poly(dA-dT) > poly(dA).poly(dT) > poly(dG-dC).poly(dG-dC) > poly(dG).poly(dC). Preference of SPM and its analogue NASPM towards the AT sequences over the GC sequences was proved from this study.

The difference in the binding of polyamines to the polynucleotides arises due to the different structural motiffs of the sequence specific polynucleotides. Poly(dA-dT).poly(dA-dT) has a classical B-form structure while poly(dA).poly(dT) has a non-standard structure with a distinct narrow minor groove and wider major groove than the usual B-form that results in a rigid bent structure and this rigidity arises from high propeller twist of the base pairs.[42,43] Furthermore, this polynucleotide has a unique spine of energetically favourable water of hydration in the narrow

groove. The binding of many small molecule intercalators which was entropy driven has been hypothesized to arise from release of water molecules from DNA.[42,44,45]

The binding of SPM and NASPM to all the polynucleotides was driven by large positive standard molar entropy changes and relatively small negative standard molar enthalpy changes clearly revealing entropy driven binding. The strong positive entropy term in all the interactions is suggestive of the disruption and release of water molecules on interaction with the helical double stranded polynucleotides. The ITC data thus suggests AT specificity for the binding of both SPM and NASPM. Also, the binding of NASPM to hetero AT polynucleotide was endothermic and found to be of higher order than that of the SPM.

Temperature dependence of the binding: Heat capacity changes

The constant pressure standard molar heat capacity change (ΔC_p^o) of polyamine-polynucleotide interactions can be determined from the temperature dependence of the binding enthalpy employing the standard relationship, $\Delta C p^o = [\partial \Delta H^o / \partial \mathrm{T}]_p$. The value of ΔC_p^o provides valuable insights into the type and magnitude of forces involved in the interaction. Temperature dependent ITC experiments were conducted at three temperatures viz. 283.15, 288.15, 293.15 K. For all the systems studied the thermograms showed single binding event at all temperatures. The thermodynamic parameters evaluated at these temperatures are depicted in Table 1. For the interaction of SPM and NASPM, the binding affinity (*K*) decreased as the temperature was increased. The binding of SPM to poly(dA-dT).poly(dA-dT) and NASPM to poly(dA-dT).poly(dA-dT) and poly(dA).poly(dT) were all deduced to be endothermic where with increasing temperature, the positive ΔH^o and $T\Delta S^o$ values decreased in such a way so that the free energy change was minimal (Table 1). The thermograms resulting from interaction of SPM to poly(dA).poly(dT), and NASPM and SPM to poly(dG).poly(dC) were all exothermic where

with increase in temperature the enthalpy values increased and entropy contribution decreased without much change in the Gibbs energy. The same phenomenon was also observed for the binding of SPM and NASPM with poly(dG-dC).poly(dG-dC) as reported in Table S1 (ESI†) where with increasing temperature the ΔH^o and $T\Delta S^o$ changed in such a way so as to make the ΔG^o change minimal.

A plot of the variation of ΔH^o with temperature is presented in Fig. 4. The slope of the lines for SPM and NASPM gave values of -151.9 and -87.4 cal/mol K for poly(dA).poly(dT), -97.3, -107.3 cal/mol K for poly(dA-dT).poly(dA-dT), -60.6 and -52.9 cal/mol K for poly(dG).poly(dC) and -52.7 and -78.7 cal/mol K for poly(dG-dC).poly(dG-dC) (Tables 1 and ESI† Table S1). Negative heat capacity values are known to be the hall mark of small molecules binding to DNA and RNA.[46-50] Large, negative magnitude for standard molar heat capacity change are characteristic for specific changes in hydrophobic or polar group hydration and is considered as an indicator of dominant hydrophobic effect in the binding process. The change in solvent accessible surface area has also been shown to be a large component of $\Delta C_p{}^o$.[51,52,53] Here, the values of $\Delta C_p{}^o$ are non-zero indicating temperature dependence of the enthalpy change which suggests that the binding enthalpy becomes more favorable and binding entropy less favorable at higher temperatures. The values of $\Delta C_p{}^o$ obtained here are lower than that is generally observed for DNA and RNA intercalators and hence support the suggestion of a groove binding model with hydrophobic contribution to the binding. DNA binding and associated change in structured water in the minor groove can be associated with heat capacity changes. Release of such water of hydration accompanies the transfer of some non polar groups into groove of the helix. Nonspecific binding by small molecules like what is seen here usually has smaller $\Delta C_p{}^o$ changes.[54] The higher values of $\Delta C_p{}^o$ for the binding of the polyamines to the AT polynucleotide

suggests conformational differences in the double stranded polynucleotide structures. It is known that AT base pairs have more water of hydration as compared to GC base pairs and the differences in the release of structured water consequent to the transfer of the polyamine molecules into the interior of the groove may lead to the observed differences in the heat capacity values.

The free energy component for the hydrophobic transfer step of binding of these molecules may be evaluated from the relationship[55], $\Delta G^{o}_{hyd} = (80\pm10) \times \Delta C_{p}^{o}$. Based on this the ΔG^{o}_{hyd} values for binding of SPM and NASPM to poly(dA).poly(dT) were deduced to be -12.15, -6.99 kcal/mol, to poly(dA-dT).poly(dA-dT) were -7.78, -8.58 kcal/mol, to poly(dG).poly(dC) were -4.85 and -4.23 kcal/mol and to poly(dG-dC).poly(dG-dC) were -4.22, and -6.30 kcal/mol, respectively. These results divulge the importance of the hydrophobic interactions involved in the binding of SPM and NASPM with the double stranded DNA polynucleotides. ΔG^{o}_{hyd} values suggest the interactions to be greater with the AT polynucleotides due to higher water of hydration associated with the AT sequences. Thus, we can say that the binding thermodynamics of SPM and NASPM to DNA polynucleotides does reflect AT base pair specificity of binding. Values of ΔC_{p}^{o} support the suggestion of a groove binding model and values of ΔG^{o}_{hyd} suggest significant hydrophobic contribution to the binding. Also, the ΔG^{o}_{hyd} values for NASPM interaction was found to be highest for AT hetero polynucleotide. This showcases the specificity of NASPM towards the AT hetero polynucleotide.

Enthalpy–entropy compensation

In all the systems studied, both the reaction enthalpy and entropy that are strong functions of temperature compensated each other to make the reaction Gibbs energy more or less independent of the temperature. For the binding of SPM to poly(dA).poly(dT) with increase in temperature

the enthalpy increased and entropy decreased without much change in the Gibbs energy. Similarly for SPM and NASPM binding to poly(dA-dT).poly(dA-dT) with increasing temperature, the positive ΔH^o values decreased and $T\Delta S^o$ values also decreased in such a way so that the Gibbs energy change was minimal (Table 1). Similar phenomenon was also observed for the binding of poly(dG).poly(dC) and poly(dG-dC).poly(dG-dC) with SPM and NASPM (ESI† Table S1). A number of biomolecular interactions have been reported to exhibit this enthalpy-entropy compensation behaviour[56,57] which suggests a significant hydrophobic component to the binding energies linked to the solvent reorganization accompanying binding interactions. This occurs generally with ΔCp^o not equal to zero and $\Delta Cp^o > \Delta S^o$. In Fig. 5 the variation of ΔH^o and ΔG^o as a function of $T\Delta S^o$ is presented for SPM and NASPM binding to the AT polynucleotides. The values of slope of ΔH^o versus $T\Delta S^o$ for the binding of SPM and NASPM to poly(dA).poly(dT) were 0.99 and 0.98, to poly(dA-dT).poly(dA-dT) were 0.89, and 0.91, to poly(dG).poly(dC) were 0.96 and 0.91, and to poly(dG-dC).poly(dG-dC) were 0.67 and 0.86, respectively. Enthalpy change with $T\Delta S^o$ revealed a linear relationship with a slope near unity which is an indication of complete enthalpy-entropy compensation.

Salt dependence of the interaction profile

The interaction of SPM and NASPM to four different polynucleotides was investigated at three conditions viz. 10, 20 and 30 mM [Na$^+$]. The data was analyzed in conjunction with van't Hoff analysis that revealed the parsing of the Gibbs energy in the binding of the biogenic polyamines and NASPM. The relation between binding constant (K) and Na$^+$ ion concentration has been described previously by Record.[58] The equation is $\partial \log(K)/\partial \log([Na^+]) = -z\varphi$, where z is the apparent charge of the bound ligand and φ is the fraction of sodium ions bound per DNA phosphate group.

With the increase of salt concentration the binding affinity decreased to a considerable extent. However, the change in the number of binding sites was subtle. A plot of ln K versus ln $[Na^+]$ (Fig. 6) for SPM and NASPM was deduced to be linear and gave values of slope as $^-1.47$ and -1.02, respectively, with poly(dA).poly(dT), -1.31, -1.16, respectively, with poly(dA-dT).poly(dA-dT), -1.22, -1.39, respectively, with poly(dG).poly(dC) and -1.03, -0.95, respectively, with poly(dG-dC).poly(dG-dC).

The observed free energy can be partitioned between the polyelectrolytic (ΔG°_{pe}) and non-polyelectrolytic (ΔG°_{t}) contributions which can be derived from the dependence of K on $[Na^+]$. The contribution to the free energy from the electrostatic interaction (polyelectrolytic) can be quantitatively determined from the relationship $\Delta G^{\circ}_{pe} = -z\varphi$ $RTln[Na^+]$ and $\Delta G^{\circ} = (\Delta G^{\circ}_{pe} + \Delta G^{\circ}_{t})$, where $z\varphi$ is the slope of the van't Hoff plot. The ΔG°_{pe} contributions at 20 mM $[Na^+]$ concentration for binding of SPM and NASPM to poly(dA-dT).poly(dA-dT), have been determined to be around -3.00, -2.64 kcal/mol, respectively, which are about 38 and 31% of the total Gibbs energy. Binding to poly(dA).poly(dT) gave values -3.44, -2.52 kcal/mol, respectively, which are 39 and 31%, respectively, of the total Gibbs energy (Table 2). Fig. 7 is a pictorial representation of parsing of free energy for the interaction of SPM and NASPM to the AT polynucleotides. Similar results were also obtained for the binding of SPM and NASPM with the GC polynucleotides (ESI† Table S2). With increase in salt concentration there was reduction in the ΔG°_{pe} values with the concomitant decrease in binding affinity. Thus, this study underscores the importance of electrostatic interactions in the binding of SPM and NASPM with these polynucleotides.

Optical melting and DSC studies: Stabilization of DNA helix by SPM and NASPM

Neutralization of the phosphate charges of the polynucleotide backbone through external binding as well as the stacking interactions, H-bonding in the grooves etc. together may contribute to the enhancement of the melting temperature (T_m) of DNA polynucleotide, the temperature at which 50% of the duplex becomes single stranded. The melting profiles of the polynucleotide and their complexes with SPM and NASPM were investigated. Fig.8 (upper panels) shows UV melting profile of the polynucleotides and their complexes. All the polynucleotides showed sigmoidal curves and melting was highly cooperative and fully reversible. The melting temperatures of poly(dA).poly(dT), poly(dA-dT).poly(dA-dT), poly(dG).poly(dC) and poly(dG-dC).poly(dG-dC) at 20 mM [Na^+] were deduced to be 50.60, 45.33, 89.16 and 97.81 ^{o}C, respectively (Fig. 8 and ESI† Fig. S2). Under saturating conditions with increasing concentration of SPM and NASPM, the T_m value of all the polynucleotides remarkably increased. At saturating SPM concentration, the ΔT_m values of the poly(dA).poly(dT), poly(dA-dT).poly(dA-dT) and poly(dG).poly(dC) were enhanced by 29.65, 19.99 and 16.35 ^{o}C, respectively. At saturating NASPM concentration the ΔT_m values of poly(dA).poly(dT), poly(dA-dT).poly(dA-dT), and poly(dG).poly(dC) were 20.04, 25.63, 14.91, respectively (Table 3). The exact T_m values of poly(dG-dC).poly(dG-dC)-SPM and NASPM complexes under saturating concentration in optical melting study could not be determined as they were beyond the detectable limits of measurements of the instrument. Thus, we can state that the ΔT_m value for the interaction of NASPM was higher for poly(dA-dT).poly(dA-dT) compared to poly(dA).poly(dT) while the reverse was observed for SPM. These results correlate well with the affinity values obtained from calorimetric studies (Table 3). The effect of SPM and NASPM in the temperature range 25-120 ^{o}C was studied by DSC to further understand the nature of the thermal unfolding and the effect of binding on the denaturation profile (lower panels of Fig. 8 and ESI† Fig. S2). The thermal melting temperatures

15

and the associated van't Hoff and calorimetric enthalpies derived from these studies are depicted in Table 3. The ratio of van't Hoff enthalpy (ΔH^o_v) to calorimetric enthalpy (ΔH^o_{cal}) for the polynucleotides was near unity indicating the melting to be cooperative reversible transitions. The T_m values of the polynucleotides and their polyamine complexes under identical buffer conditions were in complete agreement to the T_m obtained from optical absorption melting experiments (Table 3). The magnitude of the ΔT_m values of SPM-polynucleotide complexes varied as poly(dA).poly(dT) > poly(dA-dT).poly(dA-dT) > poly(dG).poly(dC) > poly(dG-dC).poly(dG-dC) while that for NASPM varied as poly(dA-dT).poly(dA-dT) > poly(dA).poly(dT) > poly(dG-dC).poly(dG-dC) > poly(dG).poly(dC). The optical melting results also provided similar results (*vide supra*). Thus, from DSC studies it can be inferred that t NASPM has higher affinity for AT polynucleotides and preferred the hetero polynucleotide over the homo polynucleotide.

The extent of the stabilization also provides a semi-quantitative evaluation of the binding affinity. SPM and NASPM binding leads to strong stabilization of all the four double stranded polynucleotides since it may form cross-links through electrostatic interaction bridging to groove of the helix, which makes the double stranded helical structure more stable to heat denaturing effects.[59]

Evaluation of binding affinity from thermal melting data

The ΔT_m values usually give an insight into the binding strength and a higher ΔT_m usually suggests stronger binding affinity. To relate melting data with binding strength we calculated the binding constants of SPM and NASPM to the polynucleotides using the following relation[60]

$1/T^o_m - 1/T_m = (R/n\Delta H_{wc})\ln(1+K_{Tm}\,\omega)$ (1)

where T^o_m is the optical melting temperature of the duplex polynucleotide in the absence of the

polyamine, T_m is the melting temperature in the presence of saturating amounts of the polyamine,

ΔH_{wc} is the enthalpy of duplex polynucleotide melting obtained from the DSC experiment, R is

the gas constant, (1.9872156 cal. K^{-1} mol^{-1}), K_{Tm} is the polyamine binding constant at the T_m, ω

is the free polyamine activity that may be estimated by one half of the total polyamine

concentration, and n is the site size of the binding. The calculated apparent binding constant at

the melting temperature can be extrapolated to a reference temperature (say 293.15 K) using the

standard relationship,

$$\Delta [\ln(K_{obs})]/ \Delta (1/T) = - (\Delta H_b/R) \qquad (2)$$

where K_{obs} is the drug binding constant at the reference temperature T (in Kelvins) and ΔH_b, the

binding enthalpy which is determined from the isothermal titration calorimetry experiment (*vide*

supra). The binding constants (K_{obs}) calculated from the melting data of the polynucleotides

using the above equations for 293.15 K is presented in (Table 3). The values obtained can be

correlated to the values of K obtained from isothermal titration calorimetry.

Thus, the helix melting studies also indicate the interaction of SPM and NASPM to be AT

specific and SPM preference is revealed as poly(dA).poly(dT) > poly(dA-dT).poly(dA-dT) >

poly(dG).poly(dC) > poly(dG-dC).poly(dG-dC) and that of NASPM as poly(dA-dT).poly(dA-

dT) > poly(dA).poly(dT) >poly(dG-dC).poly(dG-dC) >poly(dG).poly(dC). The binding affinity

values were in excellent agreement with the values obtained from calorimetric studies. Thus,

again the strong affinity of NASPM with hetero AT polynucleotide was proven.

Ethidium bromide displacement studies

The interaction of both SPM and NASPM with the four polynucleotides was further investigated

using EtBr displacement assay and the results are presented in Fig. 9. As reported earlier

polyamines can displace EtBr from its complex.[33,61,62] Polyamines are not intercalating agents, but the presence of positive charge causes them to bind to the polynucleotide helix possibly by strong electrostatic interaction. EtBr is a classical intercalator and under saturating conditions it intercalates into the double stranded DNA polynucleotide structure which in turn leads to increased fluorescence of the complex. Then successive addition of polyamines to the complex allows the interaction of polyamines with the negatively charged phosphate groups of the double helical backbone. These new interactions lead to changes and modification in the helical nature of the double stranded polynucleotide thereby distorting the intercalation sites. Consequently, the intercalated EtBr molecules slip out of the intercalation site. Release of EtBr from EtBr-polynucleotide complex causes a decrease in fluorescence. This experiment is done to compare the ability of SPM and NASPM to displace EtBr from the complex which reflects the ability of polyamines to bind to the DNA polynucleotides.

From the results it can be seen that in the case of SPM the highest fluorescence decrease at low molar ratio occurred for all the four double stranded polynucleotides samples. The largest EtBr displacement was observed with poly(dA).poly(dT) followed by poly(dA-dT).poly(dA-dT) then poly(dG).poly(dC) and finally poly(dG-dC).poly(dG-dC). IC_{50} values were obtained from the fluorescence experiments which denote the concentration required to decrease the fluorescence intensity by 50%. The IC_{50} values reflect the displacing ability of polyamines in all the complexes. The IC_{50} values of SPM, binding to poly(dA).poly(dT) and poly(dA-dT).poly(dA-dT) were 5.15 and 17.96 μM, respectively. IC_{50} values of SPM, binding to poly(dG).poly(dC) and poly(dG-dC).poly(dG-dC) were 23.48 and 36.98 μM, respectively. A high value of IC_{50} indicates a lower ability to displace EtBr from double helical polynucleotide structure. The lower value for SPM highlights its higher ability to displace ethidium bromide from the complex. Thus,

the mechanism seems to be dependent on the charge and molecular length of the polyamine. Thus, from these experiments too we can infer the high binding of SPM to the AT polynucleotides.

Similar experiments were conducted for NASPM and the values obtained from the fluorescence experiments for binding to poly(dA).poly(dT), was 19.20 μM, while that to poly(dA-dT).poly(dA-dT) was 11.29 μM, to poly(dG).poly(dC) was 38.14 μM and to poly(dG-dC).poly(dG-dC) was 28.34 μM. Therefore, the ability of NASPM to displace ethidium bromide from the complex also showed AT specificity where the lowest value of $IC_{50}$was for the AT hetero polynucleotide. Here the order varied as poly(dA-dT).poly(dA-dT) > poly(dA).poly(dT) > poly(dG-dC).poly(dG-dC) > poly(dG).poly(dC). Thus this experiment affirmed the results obtained from circular dichroism, calorimetric and melting studies and once again displayed selectivity and affinity of polyamine analogue NASPM towards AT hetero polynucleotide.

Conclusions

It is known that even minor structural differences in polyamine analogues are sufficient to cause anti-proliferative activity. Even so, the uptake of polyamines in malignant cells is much higher than normal cells.[12] As seen from the structure, NASPM has the same backbone structure as SPM but is differentiated due to the presence of naphthyl group. Therefore, these structural features of NASPM may facilitate the entry of the analogue into the cell. In this report interaction of the natural polyamine SPM and its analogue NASPM have been characterized with four synthetic polynucleotides to understand the base pair specificity and the associated energetics. Firstly, circular dichroism studies showed significant perturbations in the conformation of the polynucleotides especially for NASPM binding to AT hetero polynucleotide. Also, the presence of isoelliptical points for the NASPM-polynucleotide complex suggested the

interactions to be strongly equilibrated. Secondly, from ITC studies the interaction of both SPM and NASPM revealed the binding to be much higher for AT polynucleotides. Nevertheless, SPM displayed a higher affinity for the AT homo polynucleotide whereas NASPM revealed much higher affinity towards the AT hetero polynucleotide. Furthermore, the reaction of NASPM with hetero AT polynucleotide was endothermic. It may be understood that structural differences between SPM and NASPM (Fig.1) resulted in significantly different thermodynamic parameters. Thirdly, salt dependent studies showed the binding to be influenced by salt concentration suggesting ΔG^{o}_{pe} to be a partial contributor towards the Gibbs energy value. Additionally, temperature dependent ITC studies for SPM and NASPM divulged the binding to be favored by positive entropy changes and decrease in enthalpy values. The value of ΔCp^{o} in all systems studied had negative values which revealed the importance of hydrophobic interactions in the binding phenomenon. Thus, this shows that the hydrophobic forces play as important role as the electrostatic interactions. Higher ΔG^{o}_{hyd} values for the AT polynucleotides indicated that the hydrophobic contribution in the polyamine-AT polynucleotide complexes are much larger as compared to the GC polynucleotides.

Finally, SPM and NASPM induced high thermal stabilization in the AT polynucleotides. The highest ΔT_{m} for NASPM was observed with poly(dA-dT).poly(dA-dT). The results were also corroborated from EtBr displacement studies where once again NASPM proved its efficacy by displacing EtBr from AT heteropolynucleotide complex most efficiently. Thus, the binding of NASPM disclosed specificity for hetero AT where the order varied as poly(dA-dT).poly(dA-dT) > poly(dA).poly(dT) > poly(dG-dC).poly(dG-dC) > poly(dG).poly(dC) whereas the binding affinity of SPM varied as poly(dA).poly(dT) > poly(dA-dT).poly(dA-dT) > poly(dG).poly(dC) > poly(dG-dC).poly(dG-dC).

Two important conclusions can be drawn from these studies. Firstly, both the polyamines bind with AT polynucleotides with much higher efficacy and secondly NASPM has a higher binding affinity with the hetero AT polynucleotide. This is of major significance since NASPM shifted the specificity of binding towards AT hetero polynucleotide. Consequently, the high binding affinity of NASPM may help it to compete with natural polyamines for uptake and DNA binding and may also help to create a negative feedback mechanism in the polyamine metabolism pathway, thereby bringing down the intracellular polyamine concentration in tumor cells. Therefore, NASPM can be held as a potent analogue which may have the potential to interrupt with normal polyamine function. Thus, this study gives an understanding of the underlying mechanism of DNA interaction and helps us to approach a strategy for targeting the polyamine pathway as a means of antiproliferative mechanism.

Experimental section

Materials

Spermine hydrochloride (SPM), 1-naphthyl acetyl spermine (NASPM), ethidium bromide (EtBr), poly(dA).poly(dT), poly(dA-dT).poly(dA-dT), poly(dG).poly(dC) and poly(dG-dC).poly(dG-dC) were purchased from Sigma-Aldrich Corporation (St. Louis, MO, USA). The DNA polynucleotides are all double stranded and follow the classical Watson Crick base pairing scheme. In poly(dA).poly(dT) one strand is a contiguous sequence of adenine which is base paired to a contiguous sequence of thymine. Similar sequence is also followed by the homo polynucleotide poly(dG).poly(dC) in which a contiguous strand of guanine is base paired with another contiguous strand of cytosine. In the hetero polynucleotide poly(dA-dT).poly(dA-dT) each strand has alternating sequence of adenine and thymine. This strand is base paired to another strand of alternating thymine and adenine. Similar arrangement of sequence of guanine

and cytosine is followed by poly(dG-dC).poly(dG-dC). The samples were made to uniform size of about 280 (±50) base pairs by sonication in a Labsonic sonicator (B Brown,Germany) using a needle probe of 4 mm diameter. Concentration of polyamines was determined by weighing and that of the polynucleotides spectrophotometrically, expressed in terms of molarity of base pairs using molar extinction coefficients (ε) reported in the literature.[43,62] The polynucleotide samples were suspended in the experimental buffer and kept gently stirred overnight at 4°C. The nativeness of the polynucleotide samples was confirmed from optical melting and differential scanning calorimetry experiments. All experiments except the EtBr displacement assay were done in Citrate-Phosphate (CP) buffer (20 mM Na^+), pH 7.0, containing 10 mM Na_2HPO_4. The pH was adjusted using citric acid. EtBr displacement assay was conducted in 0.01M SHE buffer, pH 7.0.[61] The buffer solutions were filtered through Millipore filters (Millipore, India Pvt. Ltd, Bangalore, India) of 0.22 μM. Salt dependent studies were performed in CP buffer, pH 7.0 containing different amounts of NaCl as required.

Apparatus and measurements

CIRCULAR DICHROISM (CD) SPECTROSCOPY. Circular dichroism measurements were carried out on a Jasco J815 spectropolarimeter (Jasco International Co., Hachioji, Japan) interfaced with a thermal programmer (425L/15) and controlled by the Jasco software in a rectangular quartz cuvette of 1 cm path length at 20±0.5°C.[63] Spectra were obtained in the 210-400 nm region using a scan speed of 200 nm/min., a bandwidth of 1.0 nm and sensitivity of 100 milli degrees. Fixed concentration (30 μM) of the polynucleotide samples was titrated with increasing concentration of the polyamines. Each spectrum was averaged from five accumulations and was base line corrected and smoothed using the spectrum analysis software of the unit. The final CD spectra were expressed in terms of molar ellipticity [θ] (deg. cm^2 $dmol^{-1}$)

of polynucleotide base pair. The calibration of the CD unit was routinely checked by ammonium d-10 camphor sulphonic acid solution.

ISOTHERMAL TITRATION CALORIMETRY. ITC experiments were performed in a MicroCal VP-ITC unit (MicroCal, Inc., Northampton, MA, USA) at 20°C. In a typical experiment, aliquots of the polyamine solution (10 µl) from a stock of 600-800 µM were injected from a 299 µL rotating syringe (254 rpm) into 1.4235 mL of the polynucleotide solution (70-150 µM) in the calorimeter cell. This protocol was required to attain saturation in the polyamine–polynucleotide titrations. Corresponding control experiments were carried out to determine the heat of dilution of the polyamines. This was done by titrating aliquots of polyamines into the buffer alone. All the solutions used in ITC experiments were degassed on the Microcal's Thermovac unit to eliminate air bubbles. The duration of each injection was 20 sec and the delay time between each injection was 240 sec. A heat burst was generated on each injection which corresponds to the power required to maintain the sample and reference cells at identical temperatures and the heat was measured from the area under the peaks. The thermograms that showed one binding event were analyzed by using single set of binding sites model of the MicroCal LLC software based on the Levenberg-Marquardt non-linear least squares curve fitting algorithm as described in details previously.[64-66] The heat associated with the control experiment was subtracted from the corresponding heat associated with the polyamine-polynucleotide injection. The resulting data were analyzed using Origin software to estimate the equilibrium constant (K), the binding stoichiometry (N) and the standard molar enthalpy change (ΔH°). The standard molar Gibbs energy change (ΔG°) and the standard molar entropy change to the binding (ΔS°), were calculated using the relationship described earlier.[66,67]

Temperature dependent ITC experiments were performed at different temperatures and the standard molar heat capacity change (ΔCp^o) values were determined from the slope of the plots of the variation of ΔH^o with temperature. Besides this standard molar enthalpy-standard molar entropy compensation plot (ΔH^o /ΔG^o versus $T\Delta S^o$) was also plotted. Salt dependent ITC studies were also done for determination of polyelectrolyte (ΔG^o_{pe}) and nonpolyelectrolyte (ΔG^o_{t}) contribution to the ΔG^o.

OPTICAL THERMAL MELTING EXPERIMENTS. Optical thermal melting curves of polynucleotides and polynucleotide–polyamine complexes were measured on the Shimadzu Pharmaspec 1700 unit equipped with the Peltier-controlled TMSPC-8 model accessory (Shimadzu Corporation, Kyoto, Japan). In a typical experiment, 20 µM of the polynucleotide sample was mixed with varying concentrations of polyamine in the degassed buffer and were loaded into the eight chamber micro optical cuvette of 1 cm path length and heated at a scan rate of 1^oC min^{-1}. The change in absorbance at 260 nm was continuously monitored until no further change occurred as revealed from the profiles. The midpoint temperature (T_m) of the transition was obtained from the maxima of the first derivative plots. Optical experiments for the complexation of polyamines with poly(dG-dC).poly(dG-dC) could not be performed as the T_m values were beyond 110^oC. The melting profiles showed no hysteresis in the absence and presence of polyamines.

DIFFERENTIAL SCANNING CALORIMETRY. The excess heat capacity was measured as a function of temperature in a Microcal VP DSC calorimeter (Microcal, LLC, Northampton, MA) to study the helix to coil transition. The instrument was thermally stabilized by repeated buffer scans at a rate of 60 ^{o}C /hour to obtain a stable base line. The samples were scanned from 25 °C to 120 °C at the same scan speed at approximately 25 psi pressure first to obtain the melting

profile of the unbound polynucleotides and then at different D/P (polyamine/polynucleotide base pair molar ratio) ratios. Each experiment was repeated twice with separate fillings. The thermograms obtained were analyzed using the in-built VP Viewer software with Origin 7.0. The DSC thermograms depicting excess heat capacity versus temperature plots were analyzed using Origin 7.0 software which gave values for the melting temperature (T_m), calorimetric (ΔH^o_{cal}) and vant Hoff enthalpies (ΔH^o_v) for the transitions as described earlier.[66,67] For a complete reversible system, $\Delta H^o_{cal} / \Delta H^o_v$ is always unity or near unity. The reversibility of the transitions was also checked by allowing the sample to cool slowly (10^oC /hour) to 25^oC and then performing a repeat scan.

ETHIDIUM BROMIDE DISPLACEMENT ASSAY. Ethidium bromide displacement assays were performed on a Shimadzu RF-5301PC fluorescence spectrometer (Shimadzu Corporation). The sample cuvette was thermostated at 20^oC. In a typical experiment first the working solution (3 mL) was prepared which contained 12 μM of the polynucleotide with 1.26 μM of EtBr. This solution was stirred and excited at 490 nm and the fluorescence emission spectrum was measured in the range 510-650 nm. The fluorescence intensity at 595 nm was noted. Thereafter, small aliquots of polyamine solutions from a concentrated stock solution were added to the cuvette, stirred, equilibrated and fluorescence intensity at 595 nm recorded. This process was continued till the fluorescence intensity quenched by 50%. To evaluate the nonspecific fluorescence decrease due to dilution factor, appropriate control experiments were performed by adding identical aliquots of buffer solution into the EtBr–polynucleotide complex. Variation of the relative fluorescence intensity at 595 nm versus polyamine concentration was plotted from which the IC_{50} values i.e. polyamine concentration required to quench the fluorescence of the EtBr-polynucleotide complex by 50%, were reported.

Acknowledgements

References

1. O. Heby, *Differentiation*, 1981, **19**, 1–20.

2. C.W. Tabor, H. Tabor, *Annu. Rev. Biochem.*, 1984, **53**, 749-790.

3. T. Thomas, T.J. Thomas, *Cell. Mol. Life. Sci.*, 2001, **58**, 244-258.

4. A.C. Childs, D.J. Mehta, E.W. Gerner, *Cell. Mol. Life. Sci.,* 2003, **60**, 1394-1406.

5. J. Jänne, H. Pös, A. Raina, *Biochim. Biophys. Acta,* 1978, **473**, 241–293.

6. E.W. Gerner, F.L. Meyskens, *Natl. Rev. Cancer*, 2004, **4**, 781–792.

7. T. Thomas, T. J. Thomas, *J. Cell. Mol. Med.*, 2003, **7**, 113–126.

8. N. Babbar, N.A. Ignatenko, R.A. Casero, Jr., and E.W. Gerner, *J. Biol. Chem.*, 2003, **278**, 47762–47775.

9. N. Seiler, F. Raul, *J. Cell. Mol. Med.*, 2005, **9**, 623–642.

10. A.E. Pegg, *Cancer Res.*, 1988, **48**, 759-774.

11. L.J. Marton, A.E. Pegg, *Annu. Rev. Pharmacol. Toxicol.* 1995, **35**, 55–91.

12. R.A. Casero, L.J. Marton, *Nat. Rev. Drug Discovery,* 2007, **6**, 373–390.

13. A. Önal, *Crit. Rev. Anal. Chem.*, 2010, **40**, 60-67.

14. Y. Li, J.L. Eiseman, D.L. Sentz, F.A. Rogers, S.S. Pan, L.T. Hu, M.J. Egorin, P.S. Callery, *J. Med. Chem.* 1996, **39**, 339–341.

15. T. Thomas, S. Balabhadrapathruni, M.A. Gallo, T.J. Thomas, *Oncol. Res.*, 2002, **13**, 123–135.

16. C.J. Bacchi, L.M. Weiss, S. Lane, B. Frydman, A. Valasinas, V. Reddy, J.S. Sun, L.J. Marton, I.A. Khan, M. Moretto, N. Yarlett, M. Wittner, *Antimicrob. Agents. Chemother.*, 2002, **46**, 55–61.

17. B. Frydman, C.W. Porter, Y. Maxuitenko, A. Sarkar, S. Bhattacharya, A. Valasinas, V.K. Reddy, N. Kisiel, L.J. Marton, H.S. Basu, *Cancer Chemother. Pharmacol.*, 2003, **51**, 488–492.

18. N.A. Ignatenko, H. Zhang, G.S. Watts, B.A. Skovan, D.E. Stringer, and E.W. Gerner, *Mol. Carcinog.*, 2004, **39**, 221–233.

19. Y. Huanga, A. Pledgiea, R.A. Casero, Jr., and N.E. Davidson, *Anti-Cancer Drugs*, 2005, **16**, 229–241.

20. R. Glaser, E.J. Gabbay, *Biopolymers,* 1968, 6, 243-254.

21. T.T. Sakai, R. Torget, I. Josephine, C.E. Freda, S.S. Cohen, *Nucleic Acids Res.*, 1975, **2** 1005-1022.

22. G.J. Quigley, M.M. Teeter, A. Rich, *Proc. Natl. Acad. Sci. USA*, 1978, **75**, 64–68.

23. M.E. McMahon, V.A. Erdmann, *Biochemistry*, 1982, **21**, 5280-5288.

24. T.J. Thomas, V.A. Bloomfield, *Biopolynucleotides,* 1985, **12**, 2185–2194.

25. R. Marquet, P. Colson, C. Houssier, *J. Biomol. Struct. Dyn.,* 1988, **6**, 205–218.

26. L. Frydman, P.C. Rossomando, V. Frydman, C.O. Fernandez, B. Frydman, K. Samejima, *Proc. Natl. Acad. Sci. USA,* 1992, 89, 9186-9190.

27. B.L. Varnado, C.J. Voci, L.M. Meyer, J.K. Coward, *Bioorg. Chem.,* 2000, **28**, 395–408.

28. H. Deng, V.A. Bloomfield, J.M. Benevides, G.J. Thomas, Jr., *Nucleic Acids Res.,* 2000, **28**, 3379-3385.

29. J. Ruiz-Chica, M.A. Medina, F. Sanchez-Jimenez, F.J. Ramrez, *Biochim. Biophys. Acta,* 2003, **1628**, 11 –21.

30. C.N. N'soukpoe-Kossi, A.A. Ouameur, T. Thomas, A. Shirahata, T.J. Thomas, H.A. Tajmir-Riahi, *Biomacromolecules,* 2008, **9**, 2712–2718.

31. C.N. N'soukpoe-Kossi, A.A. Ouameur, T. Thomas, T.J. Thomas, H.A. Tajmir-Riahi, *Biochem. Cell. Biol.*, 2009, **87**, 621-630.

32. A.A. Ouameur, P. Bourassa, H.A. Tajmir-Riahi, *RNA*, 2010, **16**, 1968–1979.

33. A. Kabir, G. Suresh Kumar, *PLOS One,* 2013, **8**, e70510.

34. R.V. Gessner, C.A. Frederick, G.J. Quigley, A. Rich, A.H.-J. Wang, *J. Biol. Chem.,* 1989, **264**, 7921-7935.

35. S. Jain, G. Zon, M. Sundaralingam, *Biochemistry*, 1989, **28**, 2360-2364.

36. D.B. Tippin, M. Sundaralingam, *J. Mol. Biol.,* 1997, **26**, 71171-1185.

37. M.C. Wahl, M. Sundaralingam, *Biopolymers*, 1997, **44**, 45-63.

38. H. Ohishi, T. Ishida, K. Suzuki, K. Grzeskowiak, M. Odoko, N. Okabe, *Nucleic Acids Symp. Ser.*, 2004, **48**, 255-256.

39. A.A. Ouameur, H.A. Tajmir-Riahi, *J. Biol. Chem.*, 2004, **279**, 42041–42054.

40. A. Takazawa, O. Yamazaki, H. Kanai, N. Ishida, N. Kato, T. Yamauchi, *Brain Research*, 1996, **706**, 173-176.

41. M. Koike, M. Iino, S. Ozawa, *Neuroscience Res.*, 1997, **29**, 27–36.

42. D.G. Alexeev, A.A. Lipanov and I. Skuratovskii, *Nature*, 1987, **325**, 821-823.

43. M. Hossain, G. Suresh Kumar, *Mol. Biosyst.*, 2009, **5**, 1311–1322.

44. J.B. Chaires, *Biochemistry*, 1983, **22**, 4204-4211.

45. K.J. Breslauer, D.P. Remeta, W.Y. Chou, R. Ferrante, J. Curry, D. Zaunczkowski, J.G. Snyder, L.A. Marky, *Proc. Natl. Acad. Sci. USA.* 1987, **84**, 8922-8926.

46. J.B. Chaires, *Biopolymers* 1997, **44**, 201–215.

47. M.M. Islam, P. Pandya, S. Kumar, G. Suresh Kumar, *Mol. Biosyst.*, 2009, **5**, 244–254.

48. M.M. Islam, Roy S. Chowdhury, G. Suresh Kumar, *J. Phys. Chem. B*, 2009, **113**, 1210–1224.

49. K. Bhadra, M. Maiti, G. Suresh Kumar, *Biochim. Biophys. Acta*, 2007, **1770**, 1071–1080.

50. A. Basu, P. Jaisankar, G. Suresh Kumar, *Bioorg. Med. Chem.*, 2012, **20**, 2498–2505.

51. J. Ren, T.C. Jenkins, J.B. Chaires, *Biochemistry*, 2000, **39**, 8439–8447.

52. K.L. Buchmuelle, S.L. Bailey, D.A. Matthews, Z.T. Taherbhai, J.K. Register, *Biochemistry*, 2006, **45**, 13551–13565.

53. B. Nguyen, J. Stanek, W.D. Wilson, *Biophys. J.*, 2006, **90**, 1319–1328.

54. F.V. Murphy, M.E. Churchill, *Structure*, 2000, **15**, R83–R89.

55. J.H. Ha, R.S. Spolar, M.T. Record, *J. Mol. Biol.*, 1989, **209**, 801–816.

56. L. Jen-Jacobson, L.E. Engler and L.A. Jacobson, *Structure*, 2000, **8**, 1015–1023.

57. J.B. Chaires, *Arch. Biochem. Biophys.*, 2006, **453**, 26-31.

58. M.T. Record, Jr., C.F. Anderson, T.M. Lohman, *Q. Rev. Biophys.*,1978, **11**, 103–178.

59. A.M. Liquori, L. Constantino, V. Crescenzi, V. Elia, E. Giglio, *J. Mol. Biol.*, 1967, **24**, 113-122.

60. D.M. Crothers, *Biopolymers*, 1971, **10**, 2147-2160.

61. P. Allegra, E. Amodeo, S. Colombatto, S.P. Solinas, *Amino Acids*, 2002, **22**, 155–166.

62. A. Kabir, M. Hossain, G. Suresh Kumar, *J. Chem. Thermodyn.*, 2013, **57**, 445–453.

63. G. Suresh Kumar, S. Das, K. Bhadra, M. Maiti, *Biorg. Med. Chem.*, 2003, **11**, 4861–4870.

64. P. Giri, G. Suresh Kumar, *Biochim. Biophys. Acta*, 2007, **1770**, 1419-1426.

65. P. Giri, G. Suresh Kumar, *Arch. Biochem. Biophys.*, 2008, **474**, 183-192.

66. A. Basu, P. Jaisankar, G. Suresh Kumar, *PLoS One*, 2013, **8**, e58279.

67. M. Hossain, A. Kabir, G. Suresh Kumar, *Dyes and Pigments*, 2012, **92**, 1376-1383.

Table 1: ITC derived thermodynamic parameters for the binding of SPM and NASPM to poly(dA).poly(dT) and poly(dA-dT).poly(dA-dT) [a]

Polyamines	Temperature (K)	K (x10^6 M^{-1})	N	$\Delta G°$ (kcal/mol)	$\Delta H°$ (kcal/mol)	$T\Delta S°$ (kcal/mol)	$\Delta C_p°$ (cal/mol K)
Poly(dA).poly(dT)							
SPM	283.15	5.75±0.06	0.049±0.003	-8.762±0.025	-0.357±0.009	8.405±0.017	
	288.15	4.02±0.07	0.067±0.007	-8.697±0.016	-0.892±0.011	7.805±0.012	-151.9±0.03
	293.15	3.28±0.18	0.112±0.004	-8.732±0.011	-1.876±0.005	6.856±0.010	
NASPM	283.15	2.18±0.19	0.439±0.002	-8.152±0.014	1.498±0.011	9.650±0.023	
	288.15	1.77±0.22	0.420±0.003	-8.211±0.025	1.049±0.013	9.274±0.015	-87.4±0.11
	293.15	1.15±0.09	0.411±0.004	-8.137±0.018	0.624±0.062	8.761±0.006	
Poly(dA-dT).poly(dA-dT)							
SPM	283.15	2.41±0.18	0.126±0.001	-8.274±0.023	1.518±0.011	9.792±0.015	
	288.15	1.02±0.07	0.167±0.001	-7.924±0.015	0.918±0.008	8.842±0.021	-97.3±0.01
	293.15	0.82±0.04	0.289±0.001	-7.923±0.014	0.545±0.003	8.468±0.011	
NASPM	283.15	4.54±0.76	0.104±0.001	-8.622±0.021	3.207±0.055	11.829±0.013	
	288.15	3.16±0.42	0.068±0.001	-8.566±0.006	2.608±0.057	11.174±0.005	-107.3±0.04
	293.15	2.12±0.34	0.067±0.002	-8.473±0.010	2.134±0.049	10.607±0.008	

[a]All the data in this table are derived from ITC experiments conducted in 20 mM [Na$^+$] CP buffer, pH 7.0 and are average of four determinations, K and $\Delta H°$ values were determined from ITC profiles fitting to Origin 7 software as described in the text. The values of $\Delta G°$ and $T\Delta S°$ were determined using the equation $\Delta G° = -RT\ln K$, and $T\Delta S° = \Delta H° - \Delta G°$. All the ITC were fit to a model of single binding sites.

Table 2: ITC derived thermodynamic parameters for the binding of SPM and NASPM to poly(dA).poly(dT) and poly(dA-dT).poly(dA-dT) at different Na$^+$ concentrations.[a]

Polyamines	[Na$^+$]	K	N	$\Delta G°$	$\Delta H°$	$T\Delta S°$	$\Delta G°_{pe}$	$\Delta G°_t$
	mM	(x10^5 M^{-1})		(kcal/mol)	(kcal/mol)	(kcal/mol)	(kcal/mol)	(kcal/mol)
Poly(dA).poly(dT)								
SPM	10	69.7±0.04	0.144±0.005	-9.234±0.014	-2.694±0.017	6.540±0.012	-4.048±0.018	-5.186±0.014
	20	32. 8±0.18	0.112±0.004	-8.792±0.011	-1.876±0.005	6.916±0.011	-3.439±0.023	-5.353±0.010
	30	13.2±0.06	0.105±0.001	-8.259±0.018	-1.376±0.014	6.883±0.015	-3.082±0.012	-5.176±0.016
	10	19.6±0.17	0.421±0.002	-8.490±0.012	0.988±0.009	7.502±0.011	-2.968±0.012	-5.522±0.010
NASPM	20	11.5±0.09	0.411±0.003	-8.178±0.021	0.624±0.052	7.554±0.005	-2.522±0.015	-5.656±0.005
	30	6.16±0.06	0.398±0.004	-7.812±0.009	0.454±0.062	7.358±0.016	-2.260±0.020	-5.552±0.003
Poly(dA-dT).poly(dA-dT)								
SPM	10	18.6±0.32	0.530±0.007	-8.459±0.054	0.846±0.015	9.306±0.012	-3.535±0.024	-4.924±0.034
	20	8.20±0.04	0.289±0.001	-7.979±0.088	0.545±0.003	8.524±0.013	-3.003±0.010	-4.975±0.029
	30	4.33±0.08	0.252±0.008	-7.605±0.039	0.403±0.018	8.008±0.022	-2.692±0.008	-4.913±0.025
NASPM	10	31.2±0.12	0.075±0.001	-8.763±0.033	2.719±0.044	11.483±0.065	-3.103±0.042	-5.659±0.035
	20	21.2±0.34	0.067±0.002	-8.536±0.029	2.134±0.049	10.670±0.022	-2.636±0.013	-5.900±0.067
	30	8.06±0.75	0.065±0.001	-7.970±0.051	1.424±0.028	9.394±0.056	-2.363±0.037	-5.606±0.043

[a]All data in this table are derived from ITC experiments conducted in CP buffer, pH 7.0, and are an average of four determinations. K and $\Delta H°$ values were determined from ITC profiles fitting to Origin 7 software as described in text. The values of $\Delta G°$ and $T\Delta S°$ were determined using the equations, $\Delta G° = -RT\ln K$, and $T\Delta S° = \Delta H° - \Delta G°$. All the ITC were fit to a model of single binding sites.

Table 3: UV optical thermal melting data and binding constants from melting data at saturating concentrations of SPM and NASPM with double stranded polynucleotides.[a]

Sample	$T_m{}^a$ (°C)	$T_m{}^b$ (°C)	ΔT_m (°C)	ΔH^o (kcal/mol)	$\Delta H^o{}_v$ (kcal/mol)	$K_{Tm}{}^c \times 10^5$ (M^{-1})	$K_{obs}{}^d \times 10^5$ (M^{-1})
Poly(dA).poly(dT)	50.82	50.60	-	5.852	5.885	-	-
SPM	79.38	80.52	29.65	10.21	338.5	18.90	32.66
NASPM	70.32	71.16	20.04	9.897	747.9	21.11	17.63
Poly(dA-dT).poly(dA-dT)	44.24	45.33	-	7.353	7.564	-	-
SPM	63.89	65.70	19.99	13.34	201.5	10.11	8.95
NASPM	69.19	71.66	25.63	22.32	174.3	49.53	28.66
Poly(dG).poly(dC)	88.45	89.16	-	15.38	15.69	-	-
SPM	105.0	105.3	16.35	29.52	279.0	4.40	7.15
NASPM	104.1	103.34	14.91	23.89	201.7	3.11	4.10
Poly(dG-dC).poly(dG-dC)	98.48	97.81	-	54.15	54.40	-	-
SPM	104.4	nd	6.25	72.01	137.8	0.48	0.76
NASPM	116.8	nd	18.65	82.24	493.7	14.36	10.75

[a]Melting stabilization of DNA (ΔT_m) in the presence of saturating amounts of polyamines are average of DSC ($T_m{}^a$)and optical melting ($T_m{}^b$) data. $K_{Tm}{}^c$ is the binding constant at the melting temperature. [d] K_{obs} is the polyamine binding constant at 20 °C determined using equations described in the text. nd: not determinable.
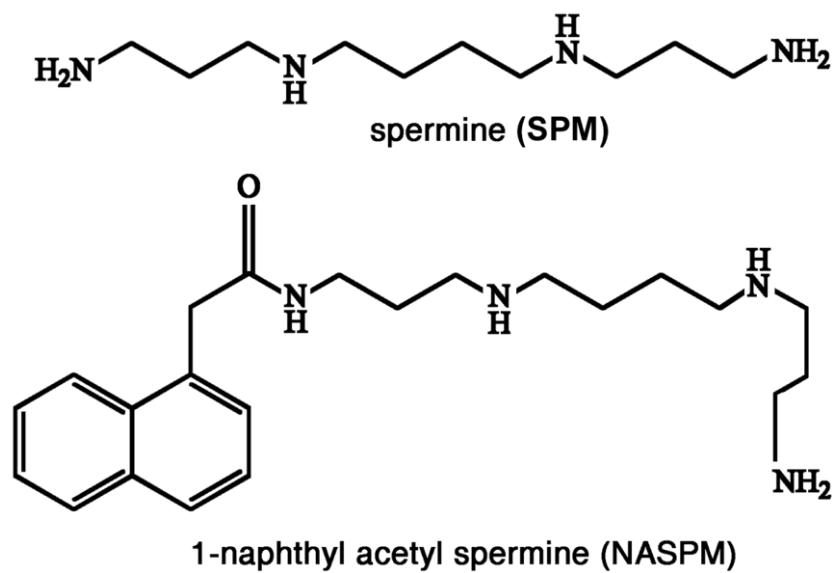
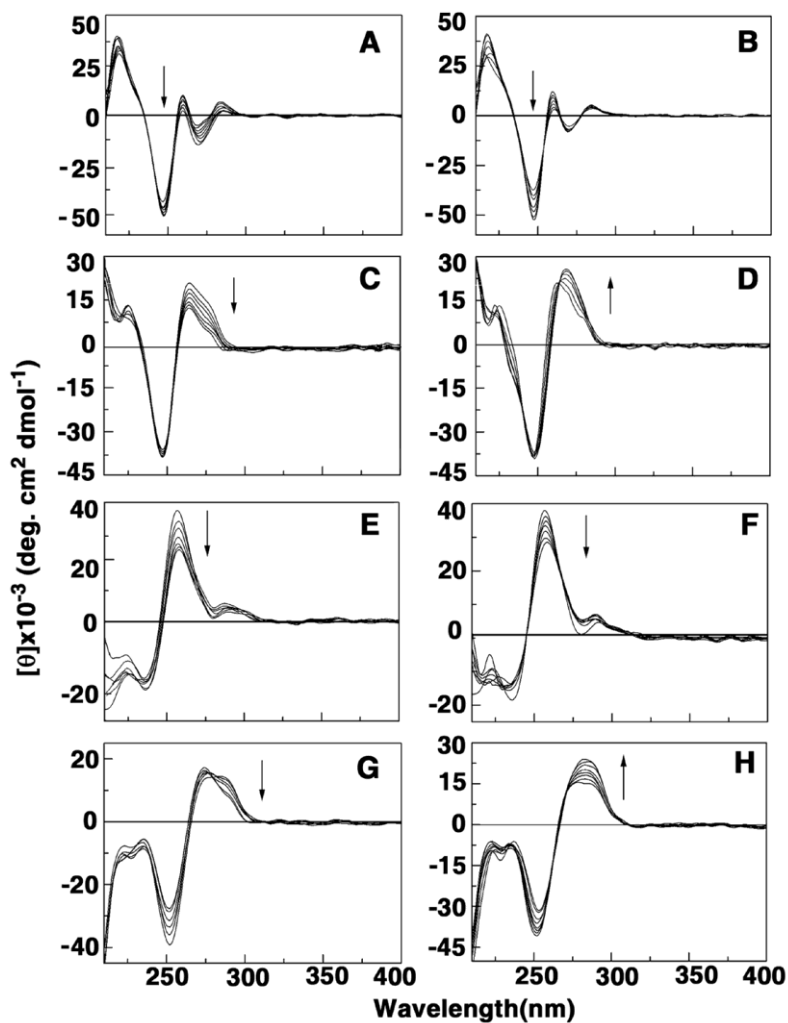**Fig. 1.** Chemical structure of spermine (SPM) and 1-naphthyl acetyl spermine (NASPM).

FIG. 2

Fig. 2. Intrinsic CD spectra for the interaction of 30 μM of (A) poly(dA).poly(dT) with SPM, (B) poly(dA).poly(dT) with NASPM, (C) poly(dA-dT).poly(dA-dT) with SPM, (D) poly(dA-dT).poly(dA-dT) with NASPM (E) poly(dG).poly(dC) with SPM (F) poly(dG).poly(dC) with NASPM (G) poly(dG-dC).poly(dG-dC) with SPM, (H) poly(dG-dC).poly(dG-dC) with NASPM, respectively. The arrows indicate spectra with varying D/P (polyamine/DNA polynucleotide) ratios from 0 to 4.
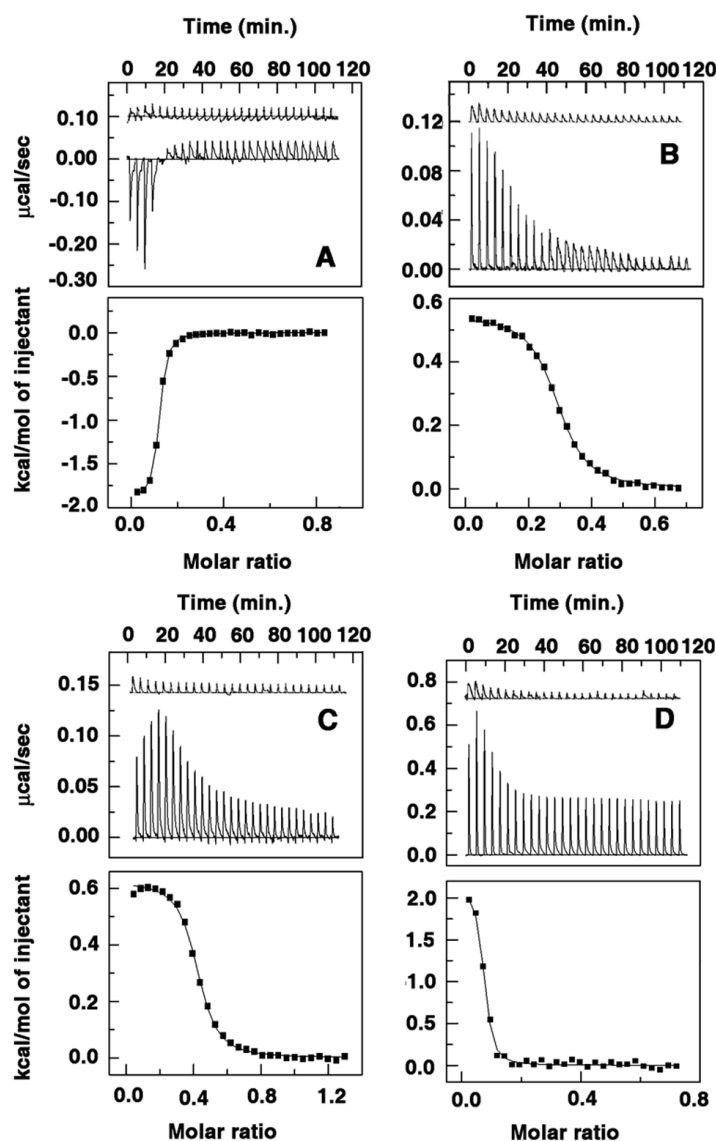
FIG. 3

Fig. 3. ITC profiles for the titration of SPM with (A) poly(dA).poly(dT) (B) poly(dA-dT).poly(dA-dT) and titration of NASPM with (C) poly(dA).poly(dT) (D) poly(dA-dT).poly(dA-dT). The top panels represent the raw data for the sequential injection of SPM and NAPSM into a solution of DNA polynucleotide and the bottom panels show the integrated heat data after correction of heat of dilution against molar ratio of DNA polynucleotide/[polyamine]. The data points were fitted to one site model and the solid line represent the best fit data.
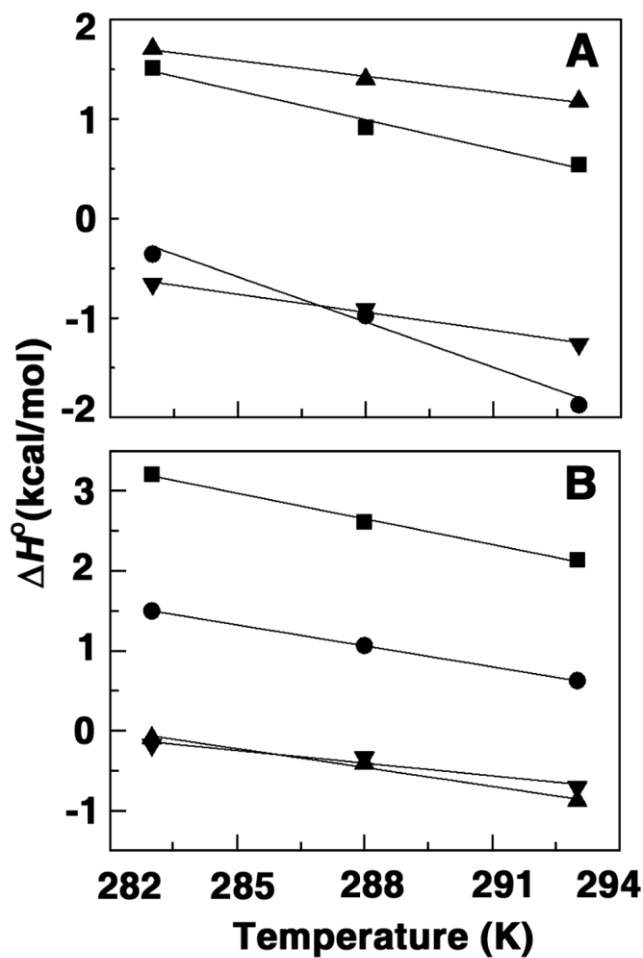
Fig. 4. Plot of variation of enthalpy of binding (ΔH^o) with temperature for the binding of (A) SPM and (B) NASPM with poly(dA).poly(dT) (●), poly(dA-dT).poly(dA-dT) (■), poly(dG).poly(dC) (▼), poly(dG-dC).poly(dG-dC) (▲).
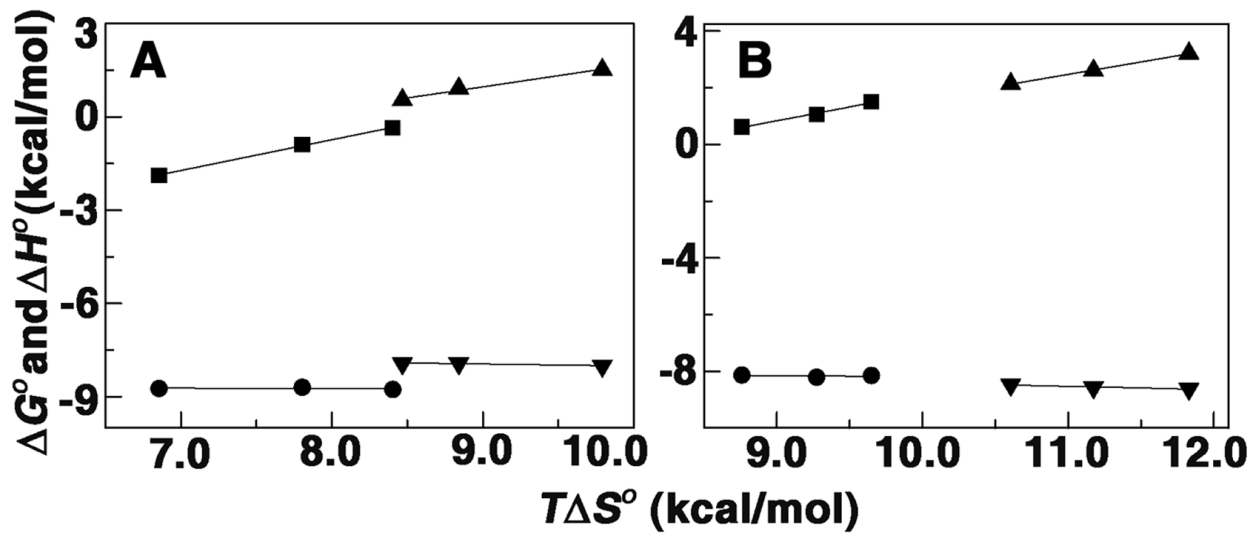
FIG. 5

Fig. 5. Plot of variation of ΔG^o and enthalpy of binding ΔH^o versus $T\Delta S^o$ for the binding of (A) SPM and (B) NASPM with poly(dA).poly(dT) ($\bullet$, $\blacksquare$), poly(dA-dT).poly(dA-dT) ($\blacktriangledown$,$\blacktriangle$).
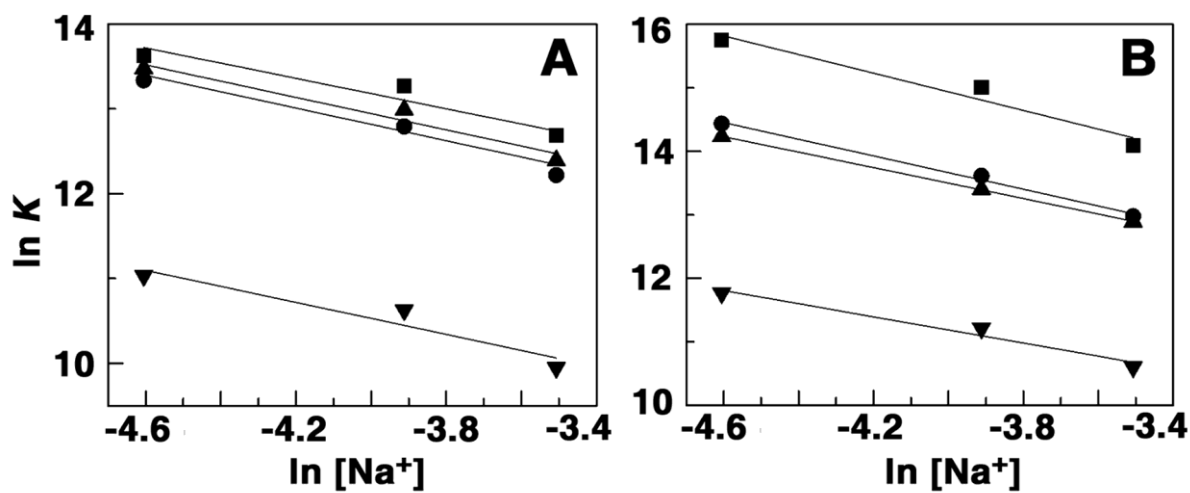
FIG. 6

Fig. 6. Plot of ln K versus ln $[Na^+]$ for the binding of (A) SPM and (B) NASPM with poly(dA).poly(dT) (■), poly(dA-dT).poly(dA-dT) (●), poly(dG).poly(dC) (▲), poly(dG-dC).poly(dG-dC) (▼) at 293.15 K.
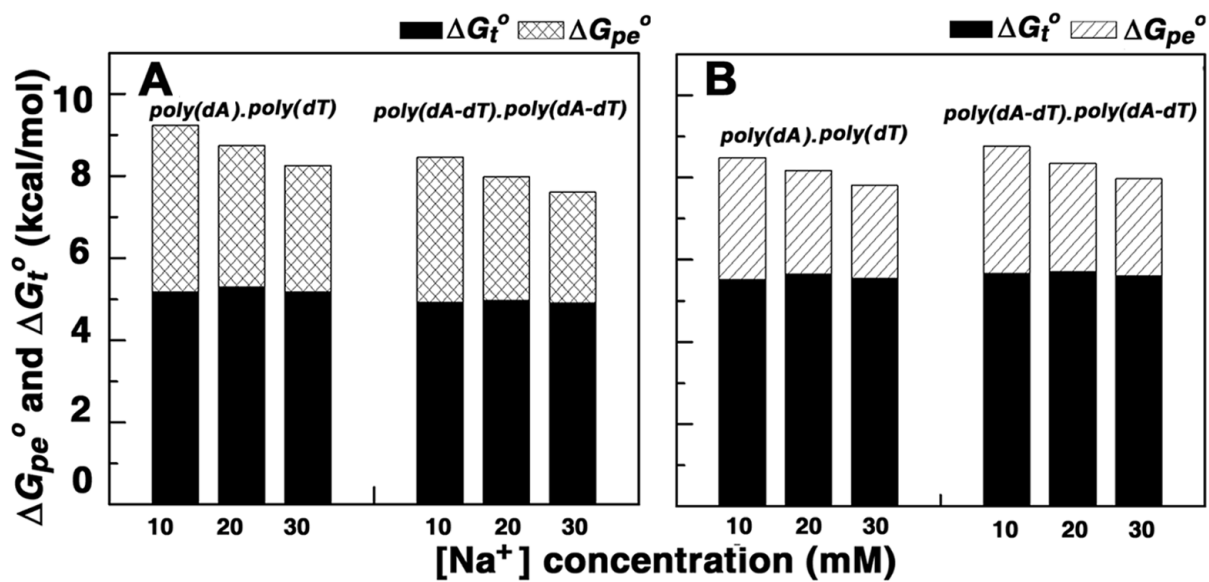
Fig. 7

Fig. 7. Non polyelectrolytic (black) (ΔG°_{t}) and polyelectrolytic (shaded) (ΔG°_{pe}) contribution for the binding of (A) SPM and (B) NASPM to AT polynucleotides.
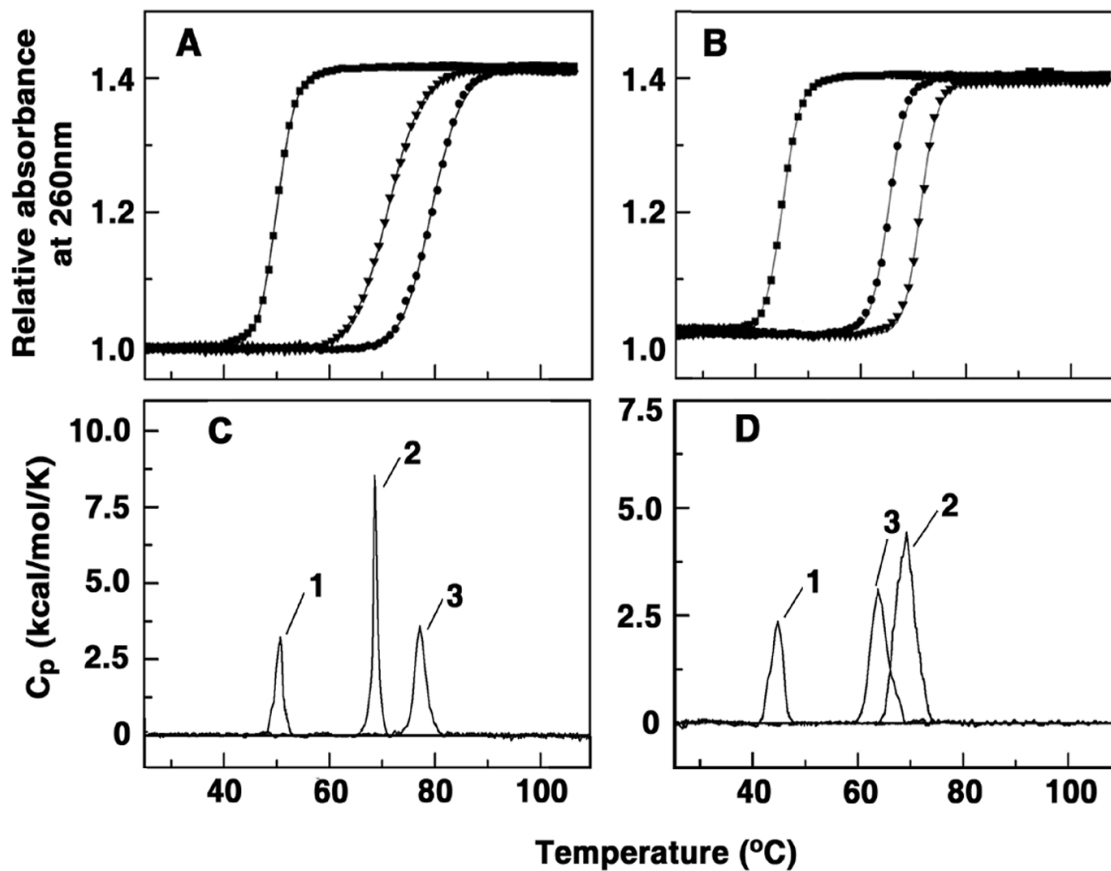
FIG. 8

Fig. 8. Optical melting profiles (upper panels) (A) poly(dA).poly(dT) (■), NASPM complex (▼), SPM complex (●), (B) poly(dA-dT).poly(dA-dT) (■), NASPM complex (▼), SPM complex (●). DSC melting profiles (lower panels) of (C) poly(dA).poly(dT) (curve 1), NASPM complex (curve 2), SPM complex (curve 3), (D) poly(dA-dT).poly(dA-dT) (curve 1), NASPM complex (curve 2), SPM complex (curve 3).
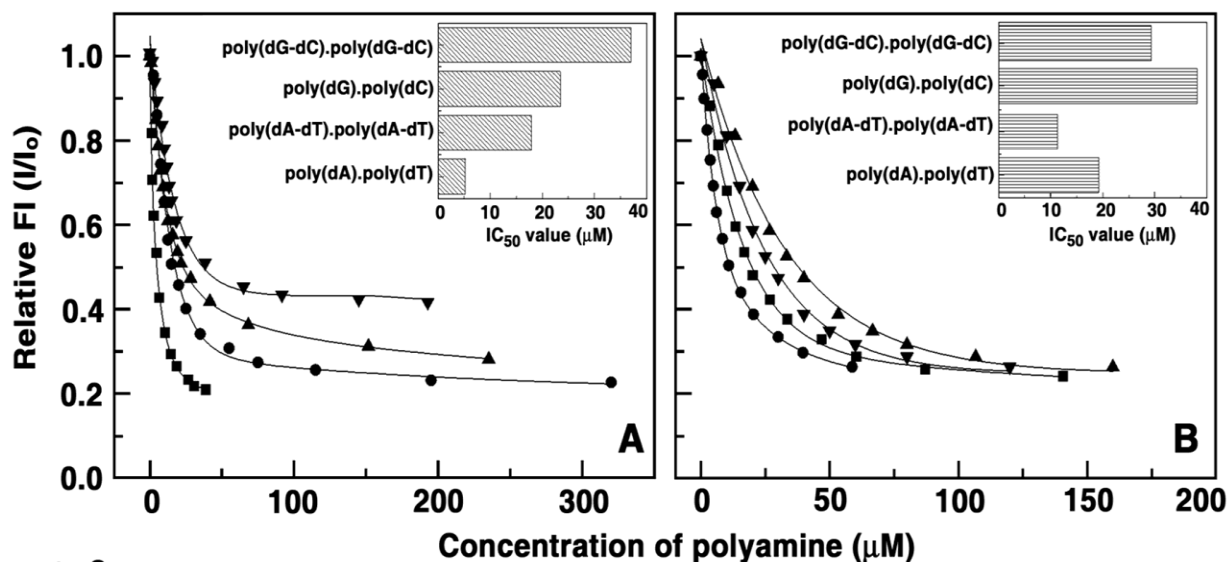
FIG. 9

Fig. 9. Relative fluorescence intensity decrease of ethidium bromide-polynucleotide complex induced by the binding of (A) SPM with poly(dA).poly(dT) (-■-), poly(dA-dT).poly(dA-dT) (-●-), poly(dG).poly(dC) (-▲-), poly(dG-dC).poly(dG-dC) (-▼-) and (B) NASPM with poly(dA).poly(dT) (-■-), poly(dA-dT).poly(dA-dT) (-●-), poly(dG).poly(dC) (-▲-),poly(dG-dC).poly(dG-dC) (-▼-) conducted in 0.01M SHE buffer pH 7.0 at 293.15 K (Inset: The values of IC_{50} of polynucleotides shown as a bar graph).